Published in final edited form as:
J Immunol. 2015 January 15; 194(2): 522–530. doi:10.4049/jimmunol.1400626.

Antigen recognition in the islets changes with progression of autoimmune islet infiltration

Robin S. Lindsay[*,†], **Kaitlin Corbin**[‡], **Ashley Mahne**[§], **Bonnie E. Levitt**[*], **Matthew J. Gebert**[*], **Eric J. Wigton**[*], **Brenda J. Bradley**[*,†], **Kathryn Haskins**[*,†], **Jordan Jacobelli**[*,†], **Qizhi Tang**[§], **Matthew F. Krummel**[‡], and **Rachel S. Friedman**[*,†]

[*]Department of Biomedical Research, National Jewish Health, Denver, CO

[†]Department of Immunology and Microbiology, University of Colorado School of Medicine, Denver, CO

[§]Department of Surgery, University of California San Francisco, San Francisco, CA

[‡]Department of Pathology, University of California San Francisco, San Francisco, CA

Abstract

In type 1 diabetes, the pancreatic islets are an important site for therapeutic intervention since immune infiltration of the islets is well established at diagnosis. Therefore, understanding the events that underlie the continued progression of the autoimmune response and islet destruction is critical. Islet infiltration and destruction is an asynchronous process, making it important to analyze the disease process on a single islet basis. To understand how T cell stimulation evolves through the process of islet infiltration we analyzed the dynamics of T cell movement and interactions within individual islets of spontaneously autoimmune non-obese diabetic (NOD) mice. Using both intra-vital and explanted 2-photon islet imaging, we defined a correlation between increased islet infiltration and increased T cell motility. Early T cell arrest was antigen dependent and due, at least in part, to antigen recognition through sustained interactions with $CD11c^+$ antigen presenting cells (APCs). As islet infiltration progressed, T cell motility became antigen-independent, with a loss of T cell arrest and sustained interactions with $CD11c^+$ APCs. These studies suggest that the autoimmune T cell response in the islets may be temporarily dampened during the course of islet infiltration and disease progression.

Introduction

Type 1 diabetes (T1D) results from the autoimmune destruction of pancreatic β-cells, primarily by autoreactive T cells. As the site of pathogenesis, the islets are the location for maintenance of the autoimmune response once infiltration begins[1]. With current diagnostic methods, treatments must be effective following disease establishment, making the islets a critical site for therapeutic intervention. Importantly, islet infiltration by immune cells is an asynchronous process, meaning that an individual pancreas can contain islet infiltration

Corresponding Author: Rachel S. Friedman, Department of Biomedical Research, National Jewish Health; Department of Immunology and Microbiology, University of Colorado, Denver, 1400 Jackson Street, K501, Denver, CO 80206, Phone: 303-270-2558, Fax: 303-398-1396, FriedmanR@NJHealth.org.

states that vary from untouched to destroyed[2]. Pooled islet analyses average this heterogeneity, potentially missing important information about key stages of the autoimmune process. Live imaging allows for the determination of cellular behaviors at distinct stages of the autoimmune response, permitting analysis of the immune response on an islet-by-islet basis.

The non-obese diabetic (NOD) mouse is regarded as the mouse model of type 1 diabetes that best replicates the human disease[3]. By four weeks of age in the NOD mouse, T cells infiltrate the pancreatic islets[4] and the pancreatic lymph nodes are no longer required for disease progression[1]. Like in the human disease, islet destruction in the NOD mouse proceeds in an asynchronous manner[3]. T cells can organize into peri-insulitic infiltrates[4] or tertiary lymphoid structures[5] prior to islet destruction. While the mechanism remains unclear, mice that are resistant to diabetes can have islet infiltration and peri-insulitis that does not progress to diabetes[6]. It is likely that peripheral tolerance mechanisms, including regulatory T cells (Tregs)[7,8], restrain the T cell mediated destruction of the β-cells during peri-insulitis. The islets are also a site of T cell stimulation, demonstrated by induction of autoreactive T cell effector function[9], and development of effector memory cells[10]. However, little is known about the series of events leading to the stimulation of T cells within the islets.

Intra-vital and explanted imaging of islets have been used in diabetes and islet transplant models. Imaging of explanted islets has been mainly used to quantify antigen-presenting cell (APC) infiltration of islets[11] and identify APC-T cell interactions within the islets[9,12]. Intra-vital islet imaging has been used to demonstrate the distinct morphology of the islet vasculature and analyze blood flow rate within the islets[13]. Using a transplant model in the anterior chamber of the eye, toxin-induced β-cell death[14], the dynamics of T cell mediated graft rejection[15], and autoimmune attack of islet transplants[16] have been analyzed. A virally induced diabetes model was used to examine the autoimmune response within the pancreas through analysis of CD8 T cell motility and interactions with β-cells[17]. This study showed direct CD8 T cell mediated killing of β-cells.

Analysis of T cell motility and interactions within the lymph node has established that increased T cell motility and aborted T cell interactions with APCs are associated with tolerance induction, whereas increased duration of T cell arrest and sustained interactions with APCs result in T cell activation[18,19,20,21]. Multiple mechanisms leading to this effect have been demonstrated in the pancreatic lymph nodes of NOD mice. Motility of T helper cells increased within antigen-bearing NOD pancreatic lymph nodes in the presence of Tregs, demonstrating that Treg-induced tolerance mechanisms are associated with increased T cell motility[7]. Also, in the NOD model, tolerance induced by transfer of antigen-pulsed, fixed APCs was broken by PD-L1 blockade. This break in tolerance resulted in T cell arrest in both the pancreatic lymph nodes and in transplanted islets[22]. Both of these studies also demonstrated that the T cell arrest in the lymph nodes was associated with increased T cell-APC interactions[7,22]. These established patterns of T cell motility within lymphoid tissue provide a baseline for understanding the significance of T cell motility changes within the islets during autoimmune attack.

We recently analyzed CD8 T cell motility and interactions with CD11c$^+$ APCs in the pancreatic islets using a model where islet infiltration was induced by transfer of OT-I T cells into RIP-mOva B6 mice[9]. This study demonstrated that in the islets, CD8 T cell motility increased, interactions with CD11c$^+$ APCs decreased, and effector cytokine production decreased with progression of islet infiltration[9]. However, overt diabetes occurred in only a minority of animals. Deletional tolerance prevents ongoing autoimmunity in the remaining animals, making it unclear whether changes in T cell motility and interactions were reflective of the reestablishment of tolerance. Additionally, since the study used very high affinity neo-antigen specific T cells, it was unclear whether the same behavior would occur using islet-antigen specific T cells in a spontaneous model of T1D. Finally, the study concluded that environmental changes caused the change in T cell behavior, but did not identify what those environmental factors were.

To further examine T cell motility and interactions with APCs within the pancreatic islets of spontaneously autoimmune NOD model of diabetes and determine the requirement for antigen, we used and validated two methods of live islet imaging by 2-photon microscopy. These techniques revealed changes in CD4 effector T cell behavior as islet infiltration progressed in the NOD model, which paralleled those observed in OT-I CD8 T cells in the RIP-mOva model, including increased T cell motility and reduced T cell arrest. Here, we further examined the role of antigen in these changes in T cell motility and interactions. In the absence of specific antigen in the islets, T cell motility was increased early in the progression of islet infiltration, suggesting that the arrest observed was a result of antigen presentation and recognition. However, the dependence on antigen as infiltration progressed was reduced. Additionally, as islet infiltration progressed, T cell-CD11c$^+$ APC contacts were decreased in duration, but not in frequency. These data support the hypothesis that T cell arrest in early stages of islet infiltration is due to T cell interactions with antigen-bearing APCs within the islets, but as islet infiltration increases environmental factors override antigen recognition leading to a loss of T cell-APC interactions within the islet.

Materials and Methods

Mice

NOD, C57Bl/6.MIP-GFP, and NOD.CD11c-YFP (Jackson #009422)[23] mice were obtained from Jackson Laboratories, NOD.BDC-2.5 T cell receptor transgenic (TCR-Tg)[24], NOD.BDC-6.9 TCR-Tg[25], and NOD.C6[25] were bred in-house by the Haskins lab. All animal procedures were approved by the IACUC committees at National Jewish Health and UCSF.

Intra-vital Surgery

Anesthesia was induced with Ketamine (50μg/g) (Vedco)/Xylazine (5μg/g) (JHP) by intra-peritoneal injection and maintained using inhaled Isoflourane (2–3% in 100% oxygen) (VetOne). 250–500μg 70kD Dextran-Rhodamine (Invitrogen) or Evans blue (Sigma) was injected intravenously to label the vasculature. Skin was removed above the surgical area and a semi-circular flap of the peritoneal wall was cut to expose the pancreas. The pancreas was manipulated with saline-soaked swabs and the area was sealed with plastic wrap to

prevent tissue desiccation, damage, and evaporative heat loss. The mouse was hydrated with subcutaneous saline and maintained at 37°C using a homeothermic warmer (Kent Scientific). The suction imaging window[26] was heated to 35–37°C and affixed using a vacuum of 25–40 mmHg to immobilize the pancreas for imaging. Islets were identified using the distinct vasculature pattern present within islets[13] (Supplemental Fig. 1). Islets that were largely destroyed lacked the distinctive vasculature pattern and were excluded from analysis. 1–5 islets per mouse were imaged from 7 mice for 16 total islets in 7 independent experiments.

Explanted Islet isolation

Islets were isolated as previously described[11,9]. Briefly mice were anesthetized with Ketamine/Xylazine prior to cervical dislocation. The pancreas was inflated with ~3 ml of 0.8 mg/ml Collagenase P (Roche) and 10 μg/ml Dnase I (Roche) in HBSS (Cellgro) via the common bile duct. Following inflation the pancreas was removed and incubated at 37°C for 10–11 min and the islets were isolated by histopaque (Sigma) density centrifugation. To ensure that the islets were intact they were handpicked under a dissecting microscope. Isolated islets were embedded in 3% low melting temperature agarose (Fisher) in DPBS. During imaging, islets were maintained at 35–37°C with flow of 95% O_2/5% CO_2 saturated RPMI (Gibco).

T cell preparation and imaging

Spleen and lymph node cells from female BDC-2.5 mice were stimulated *in vitro* with 1 μg/ml of BDC-2.5 mimetope (YVRPLWVRME) (Pi Proteomics). For studies using both BDC-2.5 and BDC-6.9 T cells, T cell stimulation was performed in vitro using 1 μg/well of plate bound anti-CD3 (BioExcel) and 2 μg/ml soluble anti-CD28 (BioExcel) antibodies. Cells were maintained in media containing 10 IU/ml rhIL-2[27] (AIDS Research and Reference Reagent Program, Division of AIDS, NIAID, NIH from Dr. Maurice Gately, Hoffmann - La Roche Inc). Day 6–14 post-activation, T cells were labeled with VPD (BD), CFSE (Invitrogen), CMTMR (Invitrogen), or eFluor670 (eBiosciences). 5×10^6 and 1×10^7 labeled cells were transferred intra-venously via the tail 48 and 24 hours prior to imaging, respectively for motility studies. For studies using only BDC-2.5 T cells transferred into WT NOD recipients, 3–5 islets per mouse were imaged from 4 mice for 16 total islets in 3 independent experiments. For studies using BDC-2.5 and BDC-6.9 co-transfers 5×10^6 peptide-stimulated BDC-2.5 T cells were transferred 48 hours prior to imaging to establish islet infiltration levels. Twenty-four hours prior to imaging 1×10^7 antibody-stimulated BDC-2.5 and BDC-6.9 T cells were co-transferred. For WT recipients 3–10 islets per mouse were imaged from 4 mice for 25 total islets in 4 independent experiments. For NOD.C6 recipients between 4–6 islets per mouse were imaged from 5 mice for 25 total islets in 5 independent experiments. An Olympus FV1000MPE 2-photon microscope[28] was used for imaging T cells in the islets. Excitation was performed at 810 nm. Imaging fields were as described[28]. Images of 27- 53 *xy* planes with 3-μm *z*-spacing were acquired every minute for 30 minutes.

Interaction Imaging

$CD4^+$ T cells from NOD.BDC-2.5 mice were selected using a negative selection kit (Stemcell). 5×10^6 dye-labeled T cells were adoptively transferred intra-venously into female NOD.CD11c-YFP recipient mice ages 9–18 weeks old. Twenty-four hours after transfer islets were isolated and imaged as described above. 2–6 islets per mouse were imaged from 5 mice for 15 total islets in 5 independent experiments.

Neutrophil and bead transfer and imaging

A custom built 2-photon microscope with published specifications[29] was used for imaging neutrophils and beads in the islets.

Neutrophils were isolated from bone marrow using a Percoll (Sigma) gradient, labeled with CMTMR (Invitrogen), and transferred retro-orbitally into B6.MIP-GFP mice immediately prior to surgery and imaging. Excitation was performed at 800nm on a 3×3 area of adjacent *z*-stacks around a representative islet. Images of up to 25 *xy* planes with 5- to 6-μm *z*-spacing were acquired every 90 or 120s for 2–3 h.

Fluorescent beads (1.75 μm, Invitrogen) were intra-venously injected into B6.MIP-GFP mice at the time of imaging. Imaging was performed at a wavelength of 800 nm on a single *xyz* plane at a rate of 30 frames per second.

Analysis

Image analysis of cells and beads was performed using Imaris (Bitplane) and MATLAB (Mathworks). Images were linearly unmixed as previously described[29]. To determine the level of islet infiltration, the region with visible transferred fluorescent T cells was manually drawn in each z plane and a total volume was determined. The infiltrated volume was then used to determine the percentage of the total islet volume that had been infiltrated. Islets were grouped into islets with mild infiltration (less than 30% of islet volume infiltrated) and advanced infiltration (between 30–60% of islet volume infiltrated). Cells within the islets tracked for ≥5 minutes were used to obtain speed, arrest coefficient, and track straightness. Cells tracked for ≥10 minutes within the islets were used to determine mean squared displacement. T cell-APC contacts were defined as a T cell and $CD11c^+$ cell spending greater than 2 min with their cell surfaces within 1 μm of each other. Sustained interactions were defined as greater than 10 min duration of contact. Statistics were calculated with Prism software (Graphpad).

Results

Immune cell dynamics in live islets can be analyzed by two imaging methods

Our goal was to analyze T cell behavior, including motility and interactions, during the progression of islet destruction in T1D. To do so we validated two methods for imaging live intact pancreatic islets by 2-photon microscopy: explanted islet imaging and a novel method of intra-vital islet imaging. Using these techniques we analyzed T cell motility in the islets of non-obese diabetic (NOD) mice, a spontaneous model of T1D. Fluorescently labeled, activated, BDC-2.5 $CD4^+$ T cells[24] were transferred into NOD mice 24 and 48 hours before

islet imaging. Data from the 24 hour T cell transfer are reported and representative of both transferred populations.

Intra-vital imaging allows the study of T cell behavior in vivo without damaging the pancreas or affecting blood flow—The pancreas was surgically exposed via a semi-circular incision through the skin and peritoneum. To stabilize the surgically exposed pancreas, we reversibly adhered an imaging window[26] to the pancreas with gentle suction and heated the window to 35°C – 37°C (Fig. 1A). This relatively simple procedure maintained the stability required for imaging with minimal force applied to the pancreas. This technique is significantly less invasive than previously established procedures for intra-vital pancreas imaging[13,17].

The islets were distinguished from the exocrine tissue based on the characteristic dense, convoluted islet vasculature[13] compared to the looser, mesh-like exocrine tissue vasculature (Fig. 1B). We confirmed that, as previously reported[13], this vasculature morphology was associated specifically with islets, by examining the islet vascular morphology in the MIP-GFP β-cell reporter mice (Supplemental Fig. 1). A collagen-rich basement membrane that surrounds the islets breaks down with advanced insulitis[30]. We were able to visualize peri-insulitic T cell infiltration inside the collagen of the intact basement membrane (Fig. 1C).

Damage to the pancreas can lead to local and systemic inflammation[31]. Previous studies using other methods of intra-vital pancreas imaging did not determine whether manipulation of the pancreas induced damage or inflammation. To determine if our imaging technique induced tissue damage, we assessed neutrophil accumulation at the imaging site (Fig. 1D, Video s1). The absence of neutrophil accumulation suggests that the pancreas remained undamaged during our imaging time frame. To determine whether blood flow was impeded by the application of the suction imaging window, we also imaged fluorescent bead motility through the blood vessels. Blood flow rates were similar to flow rates reported within the mouse pancreas[32,13], indicating that the blood flow through the islets was unimpeded by our intra-vital imaging technique (Fig. 1E, Video s2).

Imaging intact explanted islets enables analysis of large numbers of islets—Live explanted islet imaging has not been validated to ensure that in the explants T cell behavior reflects T cell activity within the intact pancreas. Isolated islets were embedded in low melt agarose and maintained at 35°C – 37°C with flow of warmed oxygenated media (Fig. 2A). Effective islet imaging was dependent upon maintaining intact islets throughout the isolation and imaging process, and was ensured by careful control of digestion time and hand picking of intact islets under a dissecting microscope (Fig. 2B). This technique allowed us to image large numbers of islets from each mouse.

T cell motility increases as islet infiltration increases

The rate of T cell motility and arrest within tissues can be used to determine whether T cells are likely to be interacting with APCs or target cells, resulting in T cell signaling. Thus, using adoptively transferred BDC2.5 T cells, T cell motility was measured within the islets to determine when T cells were likely to be receiving antigenic signals during islet infiltration (Fig. 3). Additionally using intra-venous 70kD dextran to label the blood volume,

we observed vascular leakage surrounding some infiltrated islets (Fig. 3B), which has been shown to be a prognostic indicator of pathogenic infiltration[33].

Our analysis demonstrated a correlation between T cell crawling speed and degree of islet infiltration (Fig. 3C–D). Therefore, to understand how progression of islet infiltration affected T cell behavior within the islets, we categorized islets based on stage of islet infiltration. Islets were categorized as having mild (<30% of islet volume infiltrated) or advanced (30–60% of islet volume infiltrated) infiltration (Fig. 3A–B). Islets exhibiting both infiltration levels were found within the same animal, demonstrating the heterogeneity of the islet infiltration. T cell behavior differed between individual islets of the same animal but correlated with the degree of islet infiltration.

Significant differences in T cell motility existed between mild and advanced islet infiltration (Fig. 3E Videos s3–s6). While there were small differences in crawling speed between the two imaging methods, the change in T cell behavior, indicated by the fold increase in T cell speed between mild and advanced islets, was comparable (Fig. 3E). Cellular confinement is measured by T cell track straightness, which was consistent between the explanted and intra-vital imaging methods. However, track straightness was increased in advanced versus mild-infiltrated islets, suggesting that T cells were less confined and/or they had increased directional motility with increased infiltration (Fig. 4A). Analysis of T cell arrest by the arrest coefficient (percent of time T cell speed is <2μm/min) showed that T cells in advanced islet infiltration arrested less than T cells in mild islet infiltration (Fig. 4B). The change in arrest coefficient resulted from an increased percentage of cells that were arrested for a long period of time in islets with mild infiltration (Fig. 4C), possibly due to interactions with APCs. A T cell's ability to move away from its point of origin can be analyzed by the mean squared displacement (MSD) over time. After 5 minutes, there were significant differences in the MSD between mild and advanced islet infiltration for both explanted and intra-vitally imaged islets (Fig. 4D). On the other hand, there was no significant difference in the MSD when comparing the intra-vital versus explanted methods (Supplemental Fig. 2).

The changes in T cell motility with progressing islet infiltration suggest that the islet environment is an important factor in T cell behavior in the islets. The difference in absolute speed (Fig. 3C–D) and arrest coefficient (Fig. 4B–C) between the two methods may be due to differences in available oxygen[34]. However, this did not affect the biological change in T cell motility (Fig. 3E) or the ability of T cells to translocate (Fig. 4D). These data demonstrate that the environmental factors that drive these biological changes are maintained with both imaging techniques. These data validate explanted islet imaging as a technique to examine cellular motility and interactions within the islet.

The presence of islet antigen drives T cell arrest early in islet infiltration

Based on these data and our previous data[9], it was clear that environmental factors play a critical role in the behavior of T cells in the islets as infiltration progresses; however the environmental changes driving the observed behaviors have not been elucidated. We therefore examined the presence of specific antigen as a potential environmental factor governing T cell behavior within the islets. To determine if the presence of T cell antigen was important for the arrest (Fig. 4B–C) and slow motility (Fig. 3D) observed in mild islet

infiltration, we analyzed NOD.BDC-6.9 TCR transgenic[25] T cells in the NOD.C6 mouse. The NOD.C6 mouse contains a portion of the BALB/c mouse chromosome 6, which lacks the antigen for the BDC-6.9 T cell clone[35] used to generate the NOD.BDC-6.9 TCR transgenic[25] while wild type NOD chromosome 6 contains the antigen. The NOD.C6 mouse has normal islet infiltration and diabetes incidence, but the NOD.C6.BDC-6.9 has no disease progression[25]. Utilizing the NOD.C6 as a recipient mouse we co-transferred in both BDC-2.5 T cells (for which antigen was present), and BDC-6.9 T cells (for which antigen was absent). This allowed us to determine how the presence of specific antigen affects T cell motility and arrest in the islet environment.

In wild type NOD mice BDC-6.9 T cells exhibited slower motility than BDC-2.5 T cells, but showed a similar increase in motility as infiltration increased (Fig. 5A). The slower BDC-6.9 T cell motility could be due either to higher levels of antigen for the BDC-6.9 T cells in the islets or to a higher affinity TCR for the presented antigen. However, in the NOD.C6 where the antigen for BDC-6.9 T cells was absent, BDC-6.9 T cells had higher motility compared to BDC-2.5 T cells in the same islet environment (Fig. 5B). BDC-2.5 T cells had similar motility in islets from both wild type NOD and NOD.C6, demonstrating that the islet environments were similar, while BDC-6.9 had faster motility when their antigen was absent in the NOD.C6 islets compared to wild type NOD islets (Supplemental Fig. 3).

Comparing the ratio of BDC-6.9/BDC-2.5 T cell motility within the same islet shows that in very mild infiltration (0–5% infiltrated) and advanced infiltration (30–60% infiltrated) both populations of T cells moved at similar velocities regardless of the presence of specific antigen. Notably, under conditions of very mild infiltration the T cells were largely arrested, likely due to physical confinement. On the other hand, in advanced states of infiltration, the T cells were moving quickly regardless of antigen presence.

Significantly, in islets with mild infiltration (5–30%), infiltrating BDC-6.9 T cells (No Ag) increased crawling velocity compared to BDC-2.5 T cells (+ Ag) within the same islet (Fig. 5C). This difference in motility in mild islet infiltration is due to a decrease in BDC-6.9 T cell (No Ag) arrest (Fig. 5D). The decreased BDC-6.9 arrest demonstrates that the presence of antigen is a major environmental factor that governs T cell behavior at early stages of islet infiltration.

T cell-APC interaction duration is reduced with increased islet infiltration

To determine if the antigen-dependent arrest in mild islet infiltration was due to interactions with $CD11c^+$ APCs, T cell-APC interactions were analyzed in explanted islets by 2-photon microscopy (Fig. 6). Fluorescently labeled BDC-2.5 T cells were transferred into NOD.CD11c-YFP recipient mice. We analyzed the frequency and duration of T cells that contacted $CD11c^+$ APCs in the islets. Sustained interactions, lasting longer than 10 minutes (Fig. 6A, supplemental video 7) or transient brief interactions (Fig. 6B, supplemental video 8) were present in islets with both mild and advanced infiltration. While the percentage of T cells that contacted a $CD11c^+$ APC was slightly reduced in islets with advanced infiltration (Fig. 6C), this was not significant. However, the percentage of contacts that resulted in sustained interactions (≥10 min contact) was significantly greater in islets with mild

infiltration (Fig. 6D). Additionally, the duration of T cell-APC contacts was significantly reduced in islets with advanced infiltration, further supporting the loss of sustained T cell-APC interactions (Fig. 6E). These data suggest that T cells are receiving antigenic restimulation from $CD11c^+$ APCs in islets with mild infiltration, but that these interactions along with antigenic stimulation are lost in islets with advanced infiltration.

Discussion

The data presented here in the spontaneously autoimmune NOD model of T1D, show that early in islet infiltration, antigen-dependent T cell arrest occurs which is due at least in part to antigenic interactions with $CD11c^+$ APCs. As islet infiltration progresses, these antigen-dependent sustained interactions with APCs are lost, and T cell behavior is governed by factors other than antigen. We analyzed T cells from a single adoptive transfer; however, varying degrees of endogenous autoimmune islet infiltrate were present within individual islets. T cell behavior within an animal was governed by the individual islet environment rather than the overall state of disease within the animal or the time spent within an islet. This highlights the importance of the individual islet environment, including factors such as antigen presentation and the chemokine and cytokine milieu in controlling T cell behavior within the islets.

Changes in the T cell response with T1D disease progression were not examined by the work of others studying the dynamics of the T cell response in the islets [17,15,22,12]. Our findings showing changes in T cell behavior with progression of infiltration are significant in two ways. First they suggest that antigenic T cell interactions with APCs in the islets are present in the early stages of infiltration. It is likely that these T cell interactions lead to expression of effector functions[10,9], which promote inflammation and drive entry of other cells into the islets[12,36]. Secondly, the lack of antigen recognition in the islets with increased infiltration, suggests that autoimmune T cell response in the islets may be at least temporarily dampened during the course of islet infiltration and disease progression. These data are in agreement with results analyzing the OT-I T cell response in RIP-mOva islets[9]. However, tolerance is re-established in the RIP-mOva model, so we were surprised to consistently find the same behavior in the islets of female NOD mice, considering that the incidence of disease is 75% by 40 weeks in our colony.

There are several potential explanations for why T cells lose antigenic interactions with progression of islet infiltration. Since transient T cell-APC interactions result in tolerance induction in lymph nodes[22,19,21]; it is possible that similar tolerance mechanisms occur within the islets, and this behavior represents the establishment of tolerance. Alternatively, T cells may have completed interactions with APCs and no longer require restimulation. However, data in the RIP-mOva model suggest that effector cytokine production is lost along with restimulation, suggesting that a requirement may still be present. Other possibilities include that antigen levels on APCs may be below a stimulatory threshold or the APC populations change[9] and those present within the islets are no longer able to support sustained interactions. Increased chemokine expression with islet infiltration[36] may also contribute to increased T cell motility, particularly in advanced islet infiltration where antigen presence has a reduced effect on T cell motility.

The correlation between T cell behavioral changes and islet infiltration levels in both explanted and intra-vital imaging validates these techniques for analyzing immune cell dynamics within the islets. Explanted islet imaging is a higher throughput technique that allows for the use of lower intensity fluorescent reporters. As we have shown previously, this can allow reporters such as biosensors to dynamically indicate effector function or signaling to be analyzed within the islets[9]. Intra-vital imaging allows us to investigate processes such as T cell entry into the islets[18] from the vasculature and vascular leakage, which are processes that require intact blood flow and vascular structure. Our intra-vital imaging technique also allows for the identification of the islets based on the vascular morphology, eliminating the need for a fluorescent β-cell reporter such as MIP-GFP. Examining T cell motility within islets of MIP-GFP mice is challenging since the bright signal can obscure other fluorescent cells. Eliminating the need for such reporters allows for imaging within the interior of intact islets using both of our imaging methods. By validating that both techniques provide the same readout of T cell motility at different stages of infiltration we are able to utilize the techniques for their best application.

The lack of effective treatments to halt the autoimmune response in patients with T1D may be in part due to differences in efficacy of treatment within islets at different stages of infiltration present within the same patient. This heterogeneity may leave a portion of the autoimmune response untreated in these patients. The imaging studies we present here and the studies of others[37] demonstrate the importance of examining islets on an individual basis. Examination of the heterogeneous response within the entire pancreas may hide important differences in immune response at different stages of islet infiltration. Using our imaging techniques in models of T1D, we can examine differences in T cell effector functions and activation state at different stages of disease. This approach may generate insights into the effects of therapeutic treatments and mechanisms of peripheral tolerance at different stages of the disease progression.

Supplementary Material

Refer to Web version on PubMed Central for supplementary material.

Acknowledgments

We thank Jason Lilly for islet isolation, Brianna Traxinger for animal husbandry and genotyping, and Scott Thompson for editing of the manuscript.

This work was supported by JDRF 2-2012-197 (RSF), JDRF 5-2013-200 (RSF & JJ), National Jewish Health (RSF & JJ), CRI 63003254 (RSL), JDRF 2007-170 (MFK), NIH R01 DK08231 (QT), P30 DK063720 (QT), and the Sandler Family Foundation for ongoing support (MFK).

References

1. Gagnerault MC, Luan JJ, Lotton C, Lepault F. Pancreatic Lymph Nodes Are Required for Priming of Beta Cell Reactive T Cells in NOD Mice. J Exp Med. 2002; 196:369–377. [PubMed: 12163565]
2. Bluestone JA, Herold K, Eisenbarth G. Genetics, pathogenesis and clinical interventions in type 1 diabetes. Nature. 2010; 464:1293–1300. [PubMed: 20432533]

3. Driver JP, Serreze DV, Chen YG. Mouse models for the study of autoimmune type 1 diabetes: a NOD to similarities and differences to human disease. Semin Immunopathol. 2011; 33:67–87. [PubMed: 20424843]
4. Jansen A, Homo-Delarche F, Hooijkaas H, Leenen PJ, Dardenne M, Drexhage H. Immunohistochemical characterization of monocytes-macrophages and dendritic cells involved in the initiation of the insulitis and beta-cell destruction in NOD mice. Diabetes. 1994; 43:667–675. [PubMed: 8168644]
5. Penaranda C, Tang Q, Ruddle N, Bluestone J. Prevention of diabetes by FTY720-mediated stabilization of peri-islet tertiary lymphoid organs. Diabetes. 2010; 59(6):1461–1468. [PubMed: 20299465]
6. Prochazka M, Serreze DV, Frankel WN, Leiter EH. NOR/Lt mice: MHC-matched diabetes-resistant control strain for NOD mice. Diabetes. 1992; 41:98–106. [PubMed: 1727742]
7. Tang Q, Adams JY, Tooley AJ, Bi M, Fife BT, Serra P, Santamaria P, Locksley RM, Krummel MF, Bluestone JA. Visualizing regulatory T cell control of autoimmune responses in nonobese diabetic mice. Nat Immunol. 2006; 7:83–92. [PubMed: 16311599]
8. Ott PA, Anderson MR, Tary-Lehmann M, Lehmann PV. CD4+CD25+ regulatory T cells control the progression from periinsulitis to destructive insulitis in murine autoimmune diabetes. Cell Immunol. 2005; 235:1–11. [PubMed: 16122720]
9. Friedman RS, Lindsay RS, Lilly JK, Nguyen V, Sorensen CM, Jacobelli J, Krummel MF. An evolving autoimmune microenvironment regulates the quality of effector T cell restimulation and function. Proc Natl Acad Sci U S A. 2014; 111:9223–9228. [PubMed: 24927530]
10. Chee J, Ko H, Skowera A, Jhala G, Catterall T, Graham KL, Sutherland RM, Thomas HE, Lew AM, Peakman M, Kay TWH, Krishnamurthy B. Effector-Memory T Cells Develop in Islets and Report Islet Pathology in Type 1 Diabetes. J Immunol. 2013; 192(2):572–580. [PubMed: 24337380]
11. Melli K, Friedman RS, Martin AE, Finger EB, Miao G, Szot GL, Krummel MF, Tang Q. Amplification of autoimmune response through induction of dendritic cell maturation in inflamed tissues. J Immunol. 2009; 182:2590–2600. [PubMed: 19234153]
12. Calderon B, Carrero JA, Miller MJ, Unanue ER. Cellular and molecular events in the localization of diabetogenic T cells to islets of Langerhans. Proc Natl Acad Sci U S A. 2011; 108:1561–1566. [PubMed: 21220322]
13. Nyman LR, Wells KS, Head WS, McCaughey M, Ford E, Brissova M, Piston DW, Powers AC. Real-time, multidimensional in vivo imaging used to investigate blood flow in mouse pancreatic islets. J Clin Invest. 2008; 118(11):3790–3797. [PubMed: 18846254]
14. Speier S, Nyqvist D, Cabrera O, Yu J, Molano RD, Pileggi A, Moede T, Köhler M, Wilbertz J, Leibiger B, Ricordi C, Leibiger IB, Caicedo A, Berggren P. Noninvasive in vivo imaging of pancreatic islet cell biology. Nat Med. 2008; 14:574–578. [PubMed: 18327249]
15. Abdulreda MH, Faleo G, Molano RD, Lopez-Cabezas M, Molina J, Tan Y, Echeverria OR, Zahr-Akrawi E, Rodriguez-Diaz R, Edlund PK, Leibiger I, Bayer AL, Perez V, Ricordi C, Caicedo A, Pileggi A, Berggren P. High-resolution, noninvasive longitudinal live imaging of immune responses. Proc Natl Acad Sci U S A. 2011; 108:12863–12868. [PubMed: 21768391]
16. Mojibian M, Harder B, Hurlburt A, Bruin JE, Asadi A, Kieffer TJ. Implanted islets in the anterior chamber of the eye are prone to autoimmune attack in a mouse model of diabetes. Diabetologia. 2013; 56:2213–2221. [PubMed: 23933952]
17. Coppieters K, Amirian N, von Herrath M. Intravital imaging of CTLs killing islet cells in diabetic mice. J Clin. 2012; 122:119–131.
18. Jacobelli J, Lindsay RS, Friedman RS. Peripheral tolerance and autoimmunity: lessons from in vivo imaging. Immunol Res. 2013; 55:146–154. [PubMed: 22956468]
19. Hugues S, Fetler L, Bonifaz L, Helft J, Amblard F, Amigorena S. Distinct T cell dynamics in lymph nodes during the induction of tolerance and immunity. Nat Immunol. 2004; 5:1235–1242. [PubMed: 15516925]
20. Shakhar G, Lindquist RL, Skokos D, Dudziak D, Huang JH, Nussenzweig MC, Dustin ML. Stable T cell-dendritic cell interactions precede the development of both tolerance and immunity in vivo. Nat Immunol. 2005; 6:707–714. [PubMed: 15924144]

21. Katzman S, O'Gorman WE, Villarino AV, Gallo E, Friedman RS, Krummel MF, Nolan GP, Abbas AKD. Duration of antigen receptor signaling determines T-cell tolerance or activation. Proc Natl Acad Sci U S A. 2010; 107:18085–18090. [PubMed: 20921406]
22. Fife BT, Pauken KE, Eagar TN, Obu T, Wu J, Tang Q, Azuma M, Krummel MF, Bluestone JA. Interactions between PD-1 and PD-L1 promote tolerance by blocking the TCR-induced stop signal. Nat Immunol. 2009; 10:1185–1192. [PubMed: 19783989]
23. Lindquist RL, Shakhar G, Dudziak D, Wardemann H, Eisenreich T, Dustin ML, Nussenzweig MC. Visualizing dendritic cell networks in vivo. Nat Immunol. 2004; 5:1243–1250. [PubMed: 15543150]
24. Katz JD, Wang B, Haskins K, Benoist C, Mathis D. Following a diabetogenic T cell from genesis through pathogenesis. Cell. 1993; 74:1089–1100. [PubMed: 8402882]
25. Pauza M, Dobbs C, He J, Patterson T, Wagner S, Anobile BS, Bradley BJ, Lo D, Haskins K. T-cell receptor transgenic response to an endogenous polymorphic autoantigen determines susceptibility to diabetes. Diabetes. 2004; 53(4):978–988. [PubMed: 15047613]
26. Looney MR, Thornton EE, Sen D, Lamm WJ, Glenny RW, Krummel MF. Stabilized imaging of immune surveillance in the mouse lung. Nat Methods. 2011; 8:91–96. [PubMed: 21151136]
27. Lahm H, Stein S. Characterization of recombinant human interleukin-2 with micromethods. J Chromatogr. 1985; 326:357–361. [PubMed: 3875623]
28. McKee AS, Burchill MA, Munks MW, Jin L, Kappler JW, Friedman RS, Jacobelli J, Marrack P. Host DNA released in response to aluminum adjuvant enhances MHC class II-mediated antigen presentation and prolongs CD4 T-cell interactions with dendritic cells. Proc Natl Acad Sci U S A. 2013; 110:1122–1131.
29. Bullen A, Friedman RS, Krummel MF. Two-photon imaging of the immune system: a custom technology platform for high-speed, multicolor tissue imaging of immune responses. Curr Top Microbiol Immunol. 2009; 334:1–29. [PubMed: 19521679]
30. Irving-Rodgers HF, Ziolkowski AF, Parish CR, Sado Y, Ninomiya Y, Simeonovic CJ, Rodgers RJ. Molecular composition of the peri-islet basement membrane in NOD mice: a barrier against destructive insulitis. Diabetologia. 2008; 51:1680–1688. [PubMed: 18633594]
31. Bentrem D, Joehl R. Pancreas: healing response in critical illness. Crit Care Med. 2003; 31:582–589.
32. Carlsson PO, Sandler S, Jansson L. Pancreatic islet blood perfusion in the nonobese diabetic mouse: diabetes-prone female mice exhibit a higher blood flow compared with male mice in the prediabetic phase. Endocrinology. 1998; 139:3534–3541. [PubMed: 9681505]
33. Fu W, Wojtkiewicz G, Weissleder R, Benoist C, Mathis D. Early window of diabetes determinism in NOD mice, dependent on the complement receptor CRIg, identified by noninvasive imaging. Nat Immunol. 2012; 13(4):361–368. [PubMed: 22366893]
34. Huang JH, Cárdenas-Navia LI, Caldwell CC, Plumb T, Radu CG, Rocha PN, Wilder T, Bromberg JS, Cronstein BN, Sitkovsky M, Dewhirst MW, Dustin ML. Requirements for T lymphocyte migration in explanted lymph nodes. J Immunol. 2007; 178:7747–7755. [PubMed: 17548612]
35. Dallas-Pedretri A, McDuffie M, Haskins K. A diabetes-associated T-cell autoantigen maps to a telomeric locus on mouse chromosome 6. Proc Natl Acad Sci USA. 1995; 92:1386–1390. [PubMed: 7877988]
36. Calderon B, Carrero JA, Miller MJ, Unanue ER. Entry of diabetogenic T cells into islets induces changes that lead to amplification of the cellular response. Proc Natl Acad Sci U S A. 2011; 108:1567–1572. [PubMed: 21220309]
37. Graham KL, Krishnamurthy B, Fynch S, Ayala-Perez R, Slattery RM, Santamaria P, Thomas HE, Kay TWH. Intra-islet proliferation of cytotoxic T lymphocytes contributes to insulitis progression. Eur J Immunol. 2012; 42:1717–1722. [PubMed: 22585671]

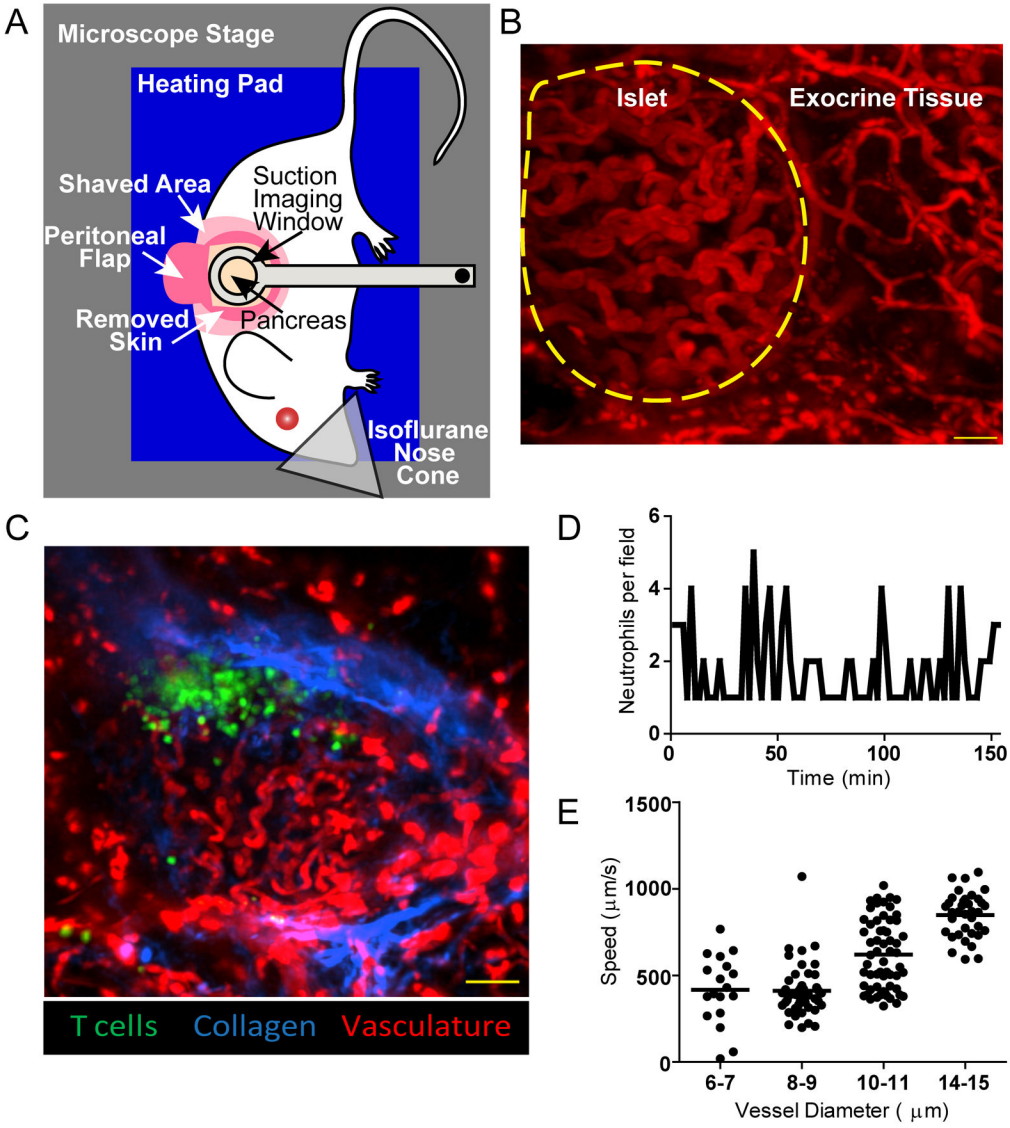

Figure 1. Intra-vital imaging maintains intact blood flow without damaging the pancreas

A) Setup for intra-vital 2-photon pancreas imaging. A heated suction window stabilizes the surgically exposed pancreas for imaging. **B–C**) Representative maximum intensity projection images of islets imaged intra-vitally through the suction imaging window captured using 2-photon microscopy. Vascular space is labeled with 70kD dextran-rhodamine (red). Images are representative of 7 experiments. **B)** Islets are identifiable by their dense convoluted vasculature compared to exocrine tissue vasculature. The border of the islet is identified with a yellow dotted line. Scale bar = 30μm. **C**) NOD mouse islet with transferred BDC-2.5 T cells (green). The collagen fluorescence is provided by the second harmonic (blue) which demonstrates that the T cell infiltration is inside the islet basement membrane. Scale bar=100μm. **D**) Neutrophils do not accumulate at the site of imaging. Fluorescently labeled neutrophils were transferred into mice prior to surgical exposure and imaging of the pancreas through the suction window. The number of neutrophils was counted every ninety seconds. The lack of neutrophil accumulation shows that the imaging

site was not damaged during imaging. Data are representative of 1 islet per mouse in 3 experiments. **E**) Suction imaging window does not impede blood flow. Fluorescent beads were tracked within blood vessels of different diameter within and around the pancreatic islets. Each dot represents one bead. Data are representative of 3 islet per mouse in 2 experiments.

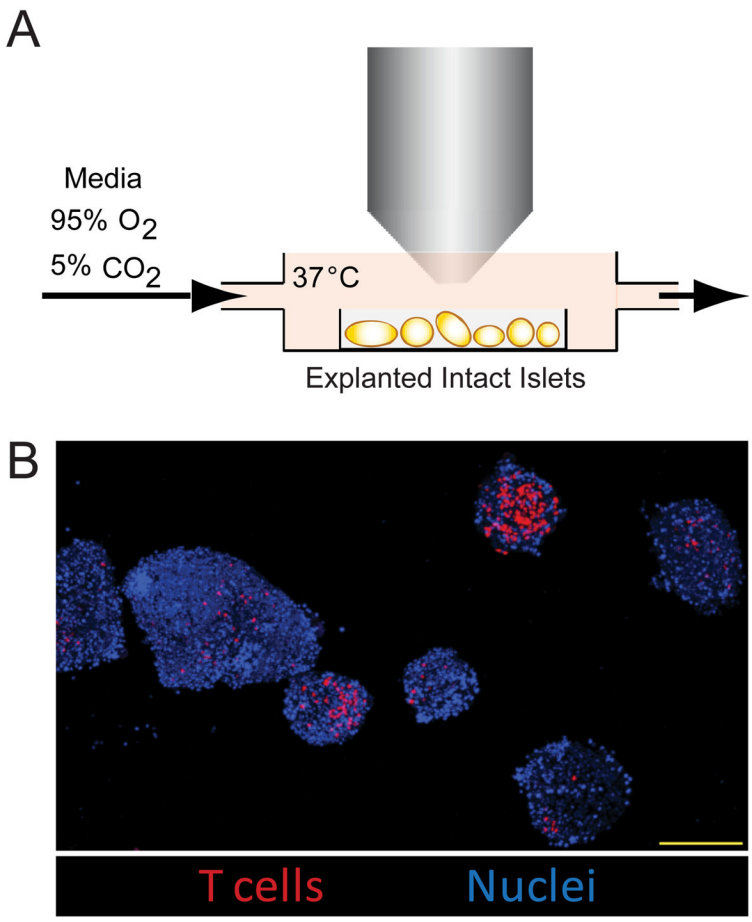

Figure 2. Explanted islet imaging allows high resolution, high throughput imaging

A) Setup of explanted islet 2-photon imaging. Isolated pancreatic islets were mounted in low melting temperature agarose and maintained at 35–37°C with constant flow of oxygenated media. **B**) Representative multiple field image of explanted islets. BDC-2.5 T cells (red) were transferred into WT NOD recipients and islets were isolated. Image shows a maximum intensity projection of explanted islets. Nuclei are labeled with Hoechst 33342 (blue). Scale bar=200μm. Images are representative of >3 experiments.

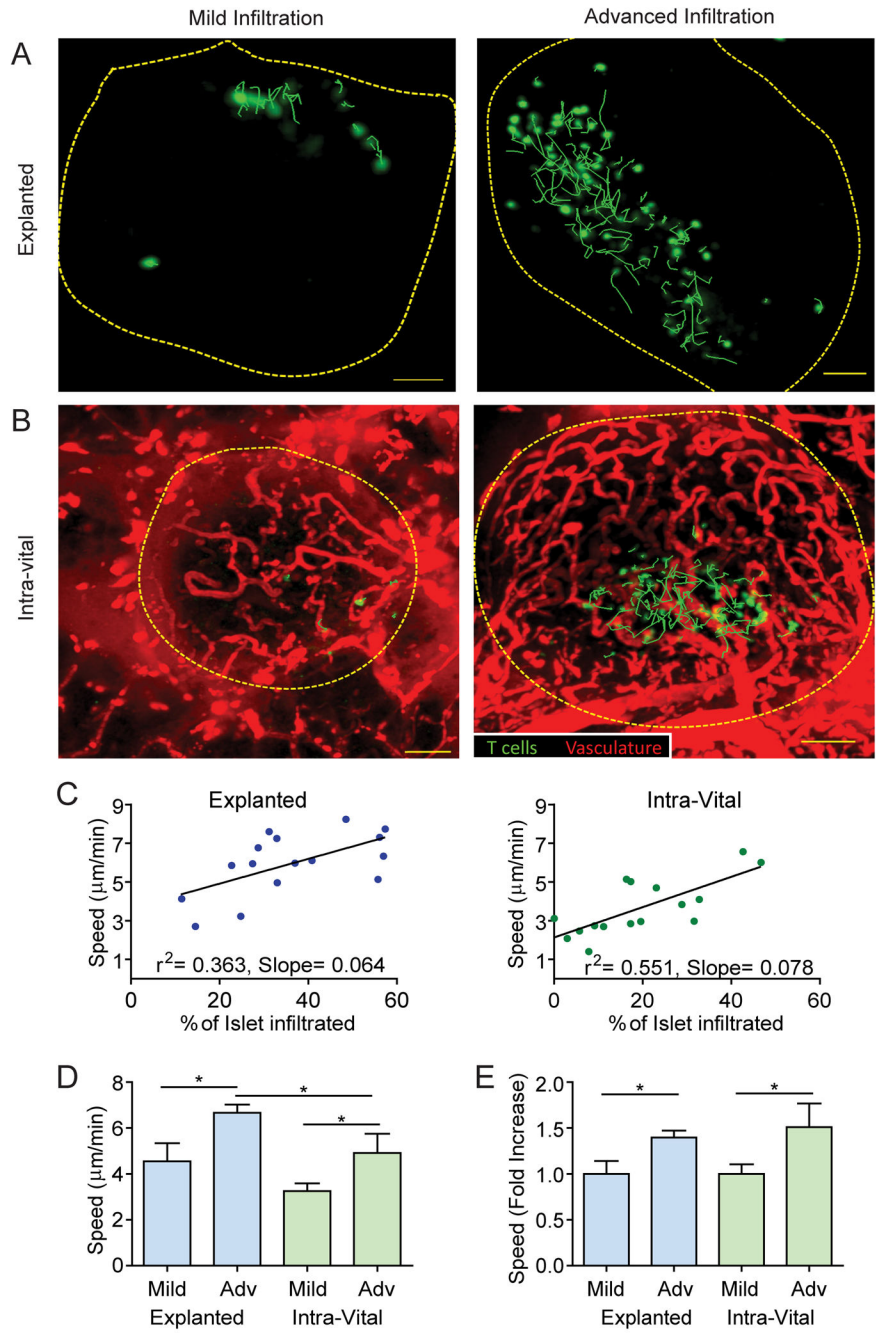

Figure 3. T cell motility increases with progression of islet infiltration

A–B) Activated BDC-2.5 T cells (green) were fluorescently labeled and transferred 24h prior to imaging. Representative maximum intensity projection images from explanted (**A**) or intra-vital (**B**) islets captured using 2-photon microscopy. Dashed lines represent the islet border. Green lines represent 10 minute paths of BDC-2.5 T cell movement. Images are representative of islets with mild infiltration (less than 30% of islet volume infiltrated) or advanced infiltration (30–60% of islet volume infiltrated). Scale bars= 50μm. **C–E)** Quantification of T cell motility within explanted or intra-vital islets. Data pooled from 16

explanted islets from 4 mice in 3 independent experiments and 16 intra-vital islets from 7 mice in 7 independent experiments. *=P<0.05, **=P<0.01; measured by Student's t test. **C**) Linear correlation of the average T cell velocity within an islet versus the percentage of the infiltrated islet volume. Each dot represents the average of all of the tracked T cells within a single islet. **D–F)** Average of individual islets. **D**) T cell crawling speed in explanted vs. intra-vital islets. **E**) Fold increase in crawling speed between islets with mild and advanced infiltration.

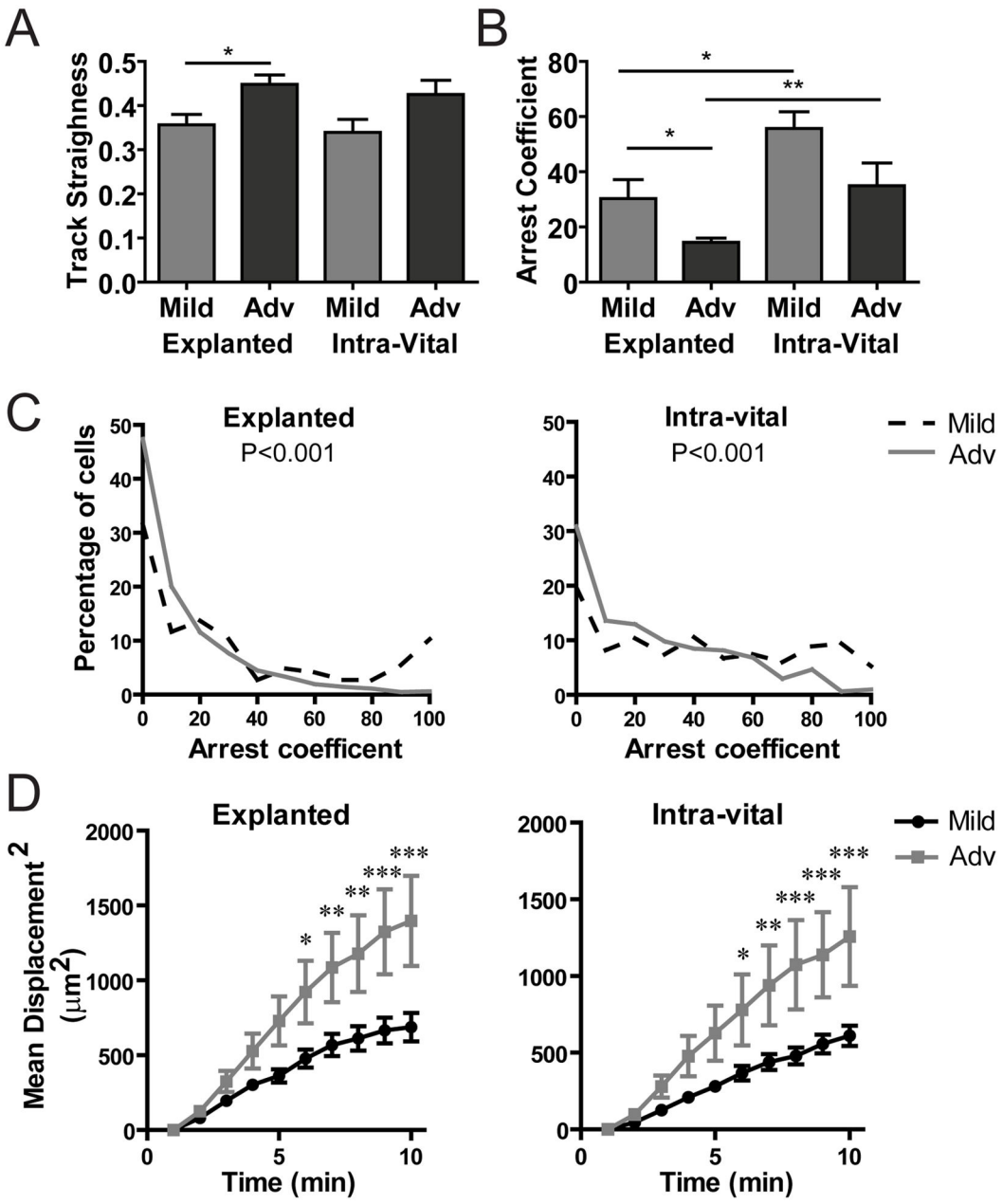

Figure 4. T cells reduce arrest and increase displacement as islet infiltration progresses

Activated BDC-2.5 T cells were fluorescently labeled and transferred 24 hours prior to imaging as in Figure 3. Data were pooled from 16 explanted islets from 4 mice in 3 independent experiments and 16 intra-vital islets from 7 mice in 7 independent experiments. *= P<0.05, **= P<0.01, ***= P<0.001; measured by 2-way Anova with Bonferroni posttests or Student's t test. **A–B)** Average of individual islets. **A**) T cell track straightness (1= cell moves in a straight line). **B–C**) T cell arrest coefficient (% of time crawling speed is <2μm/min). **D**) Mean squared displacement (μm^2) over time.

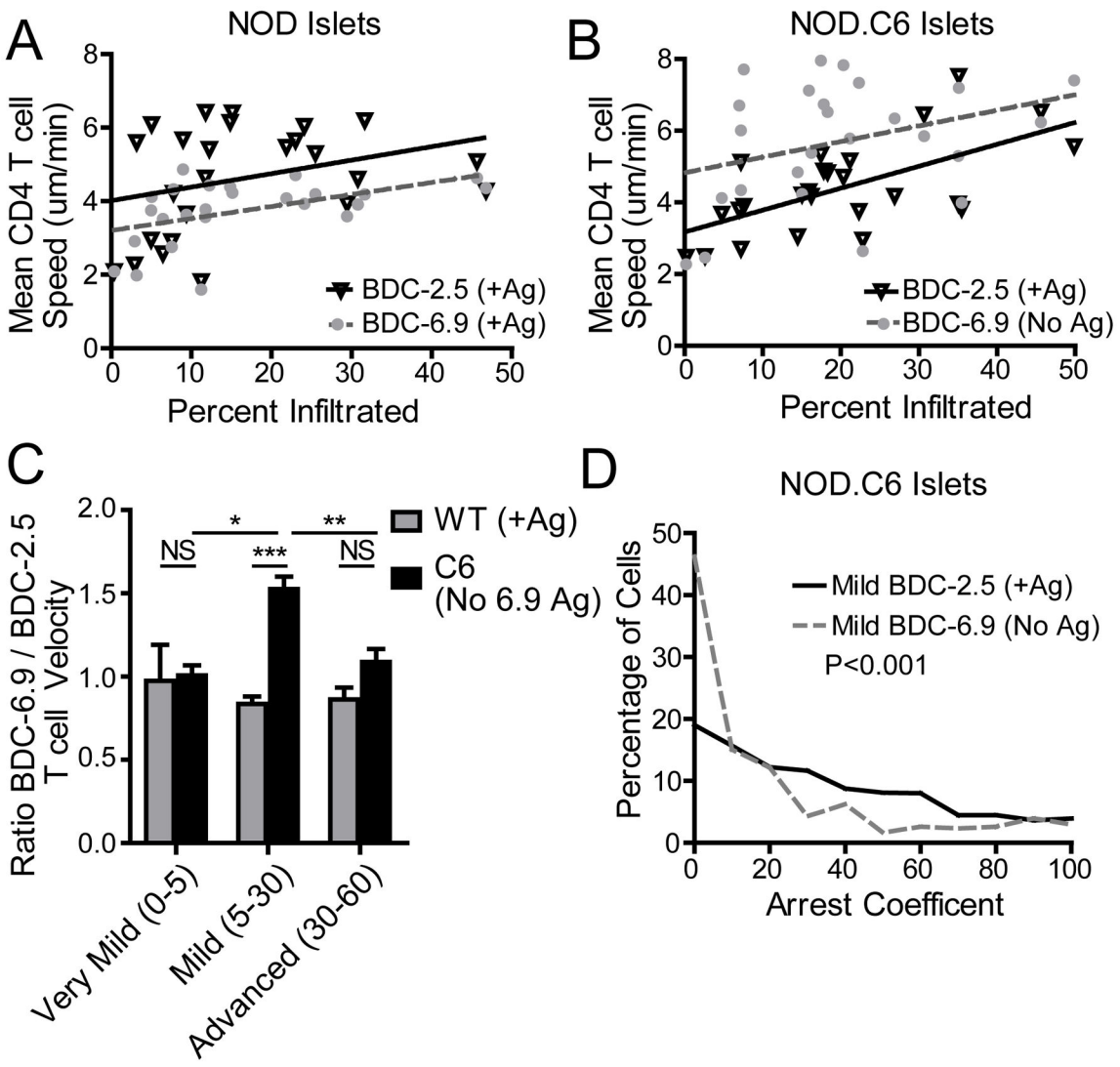

Figure 5. Early T cell arrest is antigen dependent

BDC-2.5 T cells were fluorescently labeled and transferred into WT NOD or NOD.C6 recipient mice 48 hours prior to imaging to determine infiltration state. BDC-6.9 T cells and BDC-2.5 T cells were co-transferred 24 hours prior to imaging to determine T cell motility. The antigen for BDC-6.9 T cells is absent in the NOD.C6 recipients. Data represent 25 wild type islets from 4 mice in 4 experiments and 25 NOD.C6 islets from 5 mice in 5 experiments. Each point represents the average T cell motility within 1 islet. **= P<0.01, ***= P<0.001 by two-tailed Student's t test. **A**) In WT NOD islets where the antigen was present for BDC-2.5 and BDC-6.9 T cells, both types of T cells increase motility at a similar rate as islet infiltration increases. **B**) In NOD.C6 islets, where the antigen is present for BDC-2.5 T cells, but absent for BDC-6.9 T cells, the BDC-6.9 T cells move faster in the absence of their antigen. **C**) The ratio of average BDC-6.9 T cell motility to the average BDC-2.5 T cell motility within the same islet. Infiltration states: very mild (0–5%), mild (5–30%), and advanced (30–60%). **D**) Comparison of the arrest coefficient of all BDC-2.5 and

BDC-6.9 T cells within islets with mild infiltration from NOD.C6 mice. BDC-6.9 T cells (No Ag) have reduced arrest.

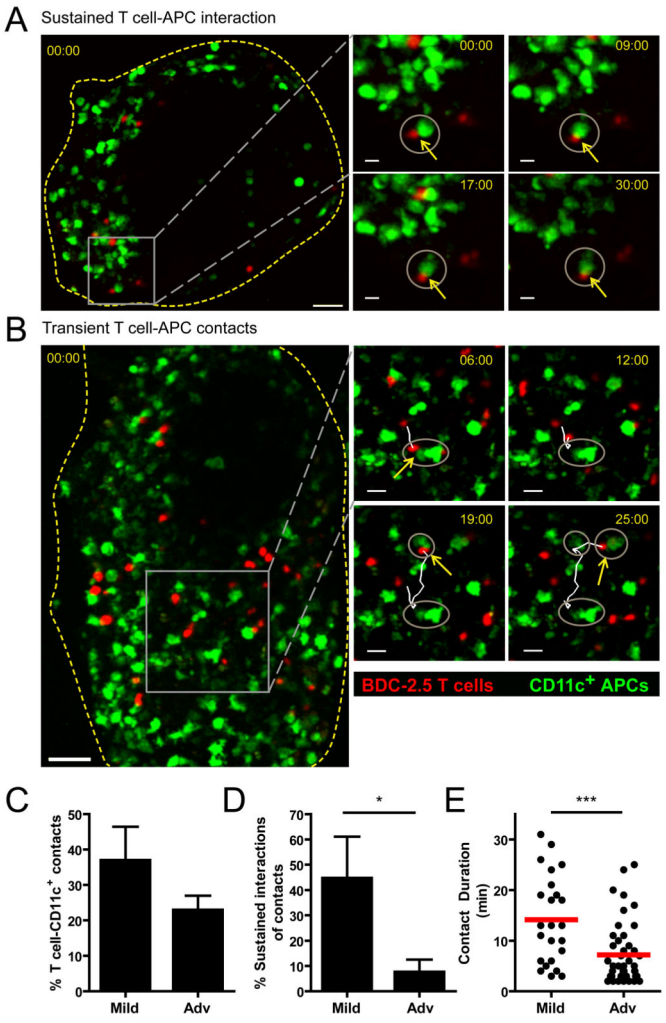

Figure 6. Sustained T cell-CD11c$^+$ APC interactions are lost with progression of islet infiltration

Fluorescently labeled BDC-2.5 T cells were transferred into CD11c-YFP hosts 24 hours prior to islet isolation and imaging. Data represent 15 islets from 5 mice in 5 independent experiments. ***= P<0.001 by two-tailed Student's t test. **A–B**) Maximum intensity projection images showing BDC-2.5 (red) and CD11c$^+$ APCs (green) within pancreatic islets. Yellow box indicates the region shown in time-lapse images on the right. Grey circles highlight the CD11c$^+$ APCs that the T cell of interest has contacted; yellow arrows show current T cell-APC contacts. Time stamps= min:sec. **A**) Sustained T cell-APC interaction in an islet with mild infiltration. Scale bar= 40μm for whole islet and 10μm for time-lapse images. **B**) Transient T cell contacts with different CD11c$^+$ APCs in an islet with advanced infiltration. Scale bar= 50μm for whole islet and 20μm for time-lapse images. **C**) Average percentage of T cells within individual islets that contact CD11c+ APCs for at least 2 min. **D)** Average percentage of T cells that contacted CD11c$^+$ APCs, which had sustained interactions of ≥ 10 min. **E**) Duration of T cell- CD11c$^+$ APC contacts.